



Published in final edited form as:

Nature. 2010 November 25; 468(7323): 533–538. doi:10.1038/nature09623.

Structure and Control of the Actin Regulatory WAVE Complex

Zhucheng Chen^{1,2}, Dominika Borek^{1,4}, Shae B. Padrick^{1,2,4}, Timothy S. Gomez³, Zoltan Metlagel^{1,2}, Ayman Ismail^{1,2}, Junko Umetani^{1,2}, Daniel D. Billadeau³, Zbyszek Otwinowski¹, and Michael K. Rosen^{1,2}

¹Department of Biochemistry, University of Texas Southwestern Medical Center at Dallas, 5323 Harry Hines Boulevard, Dallas, Texas 75390, USA

²Howard Hughes Medical Institute, UT Southwestern Medical Center, Dallas, TX 75390, USA

³Division of Oncology Research, Schulze Center for Novel Therapeutics, College of Medicine, Mayo Clinic, 200 First Street SW, Rochester, MN 55905, USA

Abstract

Members of the Wiskott-Aldrich Syndrome Protein (WASP) family control cytoskeletal dynamics by promoting actin filament nucleation by the Arp2/3 complex. The WASP relative, WAVE, regulates lamellipodia formation within a 400 kDa, hetero-pentameric WAVE Regulatory Complex (WRC). The WRC is inactive toward the Arp2/3 complex, but can be stimulated by the Rac GTPase, kinases and phosphatidylinositols. We report the 2.3 Å crystal structure of the WRC and complementary mechanistic analyses. The structure shows that the activity-bearing VCA motif of WAVE is sequestered by a combination of intramolecular and intermolecular contacts within the WRC. Rac and kinases appear to destabilize a WRC element that is necessary for VCA sequestration, suggesting how these signals stimulate WRC activity toward the Arp2/3 complex. Spatial proximity of the Rac binding site and a large basic surface of the WRC suggests how the GTPase and phospholipids could cooperatively recruit the complex to membranes.

Members of the Wiskott-Aldrich Syndrome Protein (WASP) family play central roles in the control of cellular actin dynamics¹⁻³. These proteins receive information from multiple signaling pathways and respond by promoting the actin nucleating activity of the ubiquitous Arp2/3 complex. In this way, WASP proteins control actin assembly spatially and temporally in processes including cell migration, polarization, adhesion, and vesicle trafficking.

Users may view, print, copy, and download text and data-mine the content in such documents, for the purposes of academic research, subject always to the full Conditions of use:http://www.nature.com/authors/editorial_policies/license.html#terms

Correspondence to Michael K. Rosen, Michael.Rosen@utsouthwestern.edu, Telephone: 214-645-6361.

⁴Equal contributions

Author Contributions. MKR oversaw the project. ZC, AI, SBP and JU developed the WRC reconstitution. DB, ZC and ZO determined the structure of the WRC. ZC performed the biochemical experiments. DDB and TSG performed the cellular experiments. ZM performed the EM experiments. ZC, ZO and MKR analyzed the WRC structure. DB, ZC, ZO, SBP and MKR wrote the manuscript.

Supplementary Information is linked to the online version of the paper at www.nature.com/nature.

Accession Number. Atomic coordinates of the WRC have been deposited in the Protein Data Bank under accession code 3P8C.

The WASP family is defined by a conserved C-terminal VCA motif (for Verprolin-homology, Central and Acidic regions), which binds and activates the Arp2/3 complex^{1,3}. This element must be tightly regulated to ensure proper spatial and temporal control over actin assembly. In the best understood family members, WASP and N-WASP, the VCA is autoinhibited by intramolecular interactions with a regulatory element termed the GTPase binding domain (GBD)⁴. Various ligands can bind to WASP/N-WASP simultaneously, and destabilize GBD-VCA contacts, leading to activation^{1,3}. Activation of all family members appears to be restricted to membranes. Superimposed on allosteric control and coupled with membrane recruitment, the activity of WASP proteins can be substantially increased by dimerization, or more generally oligomerization/clustering at membranes⁵.

While WASP and N-WASP can exist independently in cells, WAVE proteins are constitutively associated with four additional proteins in cells: Sra1/Cyfp1, Nap1/Hem-2, Abi and HSPC300^{6,7}. The components of this ~400 kDa pentamer, termed the WAVE regulatory complex (WRC) have all been implicated in control of Arp2/3 complex-mediated actin assembly in a wide range of systems^{1,8}. Sra1/Cyfp1 also plays a distinct role in translational control^{9,10}. WAVE proteins lack an inhibitory GBD, and the mechanism of VCA regulation within the WRC is not known. The WRC can be activated by a wide range of stimuli, including the Rac GTPase and acidic phospholipids^{6,11-14}, which appear to act cooperatively at the plasma membrane^{12,14}. Furthermore, components of the WRC can be phosphorylated at numerous positions (<http://www.phosphosite.org>), with some modifications enhancing signaling activity¹⁴⁻¹⁹. The mechanisms by which ligands act individually and cooperatively to recruit and activate the WRC are not known.

Here we report the 2.3 Å crystal structure of the WRC and complementary biochemical and cell biological analyses. The combined data reveal how the WAVE VCA is inhibited within the complex and provide plausible mechanisms for WRC activation by Rac and phosphorylation, and for cooperative membrane recruitment by Rac and phospholipids. Our analyses provide an integrated picture of how the WRC orchestrates multiple signaling pathways to control actin polymerization at the plasma membrane.

Overall structure of the WRC

To facilitate crystallization of the WRC we genetically deleted the C-terminal proline-rich region and SH3 domain of Abi2, and replaced the proline-rich region of WAVE1 with an 18-residue linker. Sra1, Nap1 and HSPC300 were full-length. The resulting miniWRC is inactive toward the Arp2/3 complex but can be stimulated by Rac1-GMPPNP¹³.

Crystals of miniWRC contained one complex in the asymmetric unit and diffracted to 2.3 Å at a synchrotron light source. Phases were obtained by multiple isomorphous replacement with anomalous scattering (MIRAS) using preparations containing selenomethionine-labeled Sra1 and Nap1 (Supplementary Table 1). The final structure was refined to $R_{\text{work}}/R_{\text{free}}=18.8\%/23.7\%$. MiniWRC has an elongated shape with approximate dimensions of $200 \times 110 \times 80$ Å (Fig. 1). Two-dimensional class averages from electron micrographs of negatively stained miniWRC and full-length WRC are indistinguishable, and of similar

dimensions as the crystal structure (Supplementary Fig. 1). The structure of miniWRC is thus likely a faithful representation of the structured elements of the WRC.

MiniWRC can be delineated into two subcomplexes: an Sra1:Nap1 dimer and a WAVE1:Abi2:HSPC300 trimer (Fig. 1). Sra1 and Nap1 have homologous structures (see below) and interact extensively to create an elongated pseudo-symmetric dimer, which forms a platform for the trimer (Supplementary Fig. 2). The N-terminal helix of Sra1 links to the rest of the complex through a flexible sequence that lacks electron density (residues 23-56), and contacts an adjacent molecule in the crystal lattice (Supplementary Fig. 3). The trimer contacts the Sra1:Nap1 dimer in a tripartite manner. A long four-helix bundle created by a helix from HSPC300 (residues 14-68), two helices from Abi2 (residues 1-39 and 43-112) and a helix from WAVE1 (residues 26-81) contacts Sra1 extensively and is aligned roughly parallel to the long axis of the dimer (Supplementary Figs. 4 and 5). The most extensive contacts are made by HSPC300, which is sandwiched between Sra1 and Abi2:WAVE1 across the entire length of its helix. The 'homeo-domain homologous region' of Abi2 (residues 112-155)²⁰ adopts an extended conformation running around the rim of a large cavity on Nap1 (Supplementary Fig. 6). The C-terminus of WAVE1, including the V- and the C-regions, forms an irregular, loosely-packed chain that lies against a concave surface of Sra1 adjacent to the long side of the four-helix bundle. As detailed below, interactions of elements in the C-terminus of WAVE1 with Sra1 and each other are central to regulation of WRC activity.

The structure reveals that Sra1 and Nap1 have the same domain organization; their coordinates can be superimposed with a root mean square deviation (r.m.s.d.) of 6.9 Å for 681 Ca atoms with Dali Z-score 17.9 (Supplementary Fig. 7)²¹. Thus, they belong to the same protein family despite their low sequence identity (13%). Homology between Sra1 and Nap1 is also supported by HHpred²², which showed additional human members of this family that are similar in size: KIAA1033/SWIP and Strumpellin, with similarity extending over their entire lengths. When analyzed pair wise, SWIP is more similar to Sra1 and Strumpellin is more similar to Nap1. We and others recently reported that SWIP and Strumpellin form a pentameric complex (SHRC, for WASH Regulatory Complex) containing the proteins CCDC53 and Fam21, and another WASP family member, WASH^{23,24,25}. Within the SHRC the WASH VCA is inactive²³. HHpred and biochemical analyses suggest that CCD53, and the N-termini of WASH and Fam21 are structurally and/or functionally similar to HSPC300 and the N-termini of WAVE and Abi, respectively²³. These many similarities, coupled with the similar overall shape of the WRC and SHRC²³, suggest that the SHRC is analogously organized as a large SWIP:Strumpellin platform bound to a helical bundle of WASH:CCDC53:Fam21, with the WASH VCA sequestered by a similar mechanism.

We validated the structural organization observed in the crystal by replacing wild type WAVE2 in HeLa cells with mutants targeting the trimer interface. Mutating the WAVE-HSPC300 interface (I50D/L54D_{WAVE2}) or the WAVE-HSPC300/Abi interface (L40D/F51D_{WAVE2}) appreciably decreased co-immunoprecipitation of WAVE2 with the four other components of the WRC (Supplementary Fig. 4), consistent with structural predictions.

Mechanism of WRC inhibition

The structure explains the inhibited nature of the WRC. In the complex, the WAVE1 VCA is bound by a conserved surface of Sra1 and residues 82-184 of WAVE1, which form five helices ($\alpha 2$ - $\alpha 6$) and a series of intervening loops. This element of WAVE1 traces a meandering path across a concave surface of Sra1, and we refer to it as the “meander region” (Fig. 2a and Supplementary Fig. 8). Contacts between the meander region and Sra1 bury over 2,100 Å² (~56% of the total WAVE1-Sra1 interface; Supplementary Fig. 9). The meander sequence is highly conserved among the different WAVE proteins (Supplementary Fig. 8), as is its contact surface on Sra1, suggesting its interactions and irregular structure are conserved.

The V- and C-regions of the VCA lie on the surface of Sra1 and form two amphipathic helices (residues 500-514 and 531-543, respectively) that also pack against $\alpha 2$ and $\alpha 6$ of WAVE1, respectively (Supplementary Fig. 10). The A-region of the VCA (residues 545-559) is likely disordered, as it is not observed in the electron density. During actin filament nucleation, the V-region recruits an initial actin monomer to the nascent filament, while the C- and A-regions contribute binding energy and induce activating conformational changes in the Arp2/3 complex^{26,27}. The structure and complementary experimental data below indicate that sequestration of both the V- and the C-regions by Sra1 and the meander region of WAVE1 underlies VCA inhibition within the WRC.

Inhibition of the V-region involves a combination of contacts to actin-binding residues and induction of structure that is incompatible with actin binding (Fig. 2b). In the complex of the V-region of WAVE2 with actin²⁸, residues equivalent to 497-507 of WAVE1 form a helix that inserts into the cleft between actin subdomains 1 and 3. Residues equivalent to 508-516 are extended, and the Ile509 and Arg512 equivalents contact actin. In the structure of miniWRC, the entire V-region is helical, and the side chains of Leu 501, Leu 502, Ile 505, Ile 509 and Arg 512 are buried in the Sra1 interface, making the V-region inaccessible to actin. Sequestration of the V-region is an important contributor to WRC inhibition, as mutating V-helix contact residues Leu 841, Phe 844 and Trp 845 of Sra1 constitutively activates miniWRC toward the Arp2/3 complex (L841A/F844A/W845A_{Sra1}-miniWRC, Fig. 2d), producing branched filaments (Supplementary Fig. 11).

The C-helix is also critical for activation of Arp2/3 complex²⁹, as mutations of Val 531, Leu 535 or Arg 538 in the WAVE1 VCA reduce activity toward Arp2/3 complex by at least 50%. In the miniWRC, the C-helix buries its hydrophobic face in the Sra1- $\alpha 6$ interface (Fig. 2c, Supplementary Figs. 8 and 9). Intermolecularly, Val 531, Ala 532, Leu 535 and Ile 539 of WAVE1 make van der Waals contacts with Sra1. Intramolecularly, Val 531, Ile 534, Leu 535, Arg 538 and Val 541 of the C-helix pack against $\alpha 6$. Hence, the structure shows that the WRC sequesters C-helix residues important for activation of the Arp2/3 complex, resulting in inhibition. This mechanism is also supported by mutagenesis: perturbing contacts of the C-helix with either Sra1 (L697D/Y704D_{Sra1}-miniWRC, Fig. 2d) or the $\alpha 6$ helix (W161E/K162D_{WAVE1}-miniWRC, Fig. 2e) leads to constitutive activation of the miniWRC *in vitro*. Additionally, replacement of wild type WAVE2 with equivalent levels of the analogous $\alpha 6$ mutant (W160E/K161D_{WAVE2}) in HeLa cells does not alter the integrity

of the complex (Supplementary Fig. 4), but causes a dramatic redistribution of actin, with loss of stress fibers and assembly of filaments at the cell periphery, again consistent with constitutive activation of the WRC (Fig. 3a).

Interactions of the VCA, and perhaps the structure of the entire meander-VCA element, appear to be highly cooperative, as perturbation of either the V- or C-region contacts produces WRC activity near that of the isolated VCA (Figs. 2d and e).

Activation by Rac

Rac plays an important role in controlling actin polymerization and lamellipodia formation through activation of the WRC *in vivo*^{8,30,31}. Rac1 binds to recombinant WRC and activates it *in vitro* at micromolar concentrations under optimized assay conditions without disrupting the integrity of the complex^{13,14} (Supplementary Fig. 12). By analogy to the activation of WASP by Cdc42⁴, we reasoned that removing the VCA from the WRC would increase its affinity for Rac1. Indeed, in pull down assays immobilized GST-Rac1:GMPPNP (a GTP analog) bound a VCA-deleted WRC (WRC) to a greater extent than miniWRC (Supplementary Fig. 13). Using equilibrium dialysis we measured a dissociation constant (K_D) of 1-2 μ M for WRC. MiniWRC bound Rac with lower affinity, having K_D of 7-10 μ M (Fig. 3b). The constitutively active L697D/Y704D_{Sra1}-miniWRC (Fig. 3b) had affinity similar to that of WRC, consistent with notion that sequestration of the VCA motif competes with Rac1 binding. These results imply that Rac1 binds to the body of the WRC competitively with the VCA (either directly or indirectly), leading to activation of the complex.

To better define the Rac1 interaction surface, we searched for WRC mutants with defects in Rac1 binding. Examination of the structure of WRC identified several conserved surface patches. Mutations L697D/Y704D, L841A/F844A/W845A or E250K/Q399A of Sra1 did not perturb the binding of WRC to Rac1 (data not shown). However, Sra1 mutations C179R, R190D, M632D and E434K/F626A, severely impaired binding of WRC to Rac1 without altering the integrity of the recombinant complex (Fig. 3b and supplementary Fig. 13). These highly conserved Sra1 residues are located in a patch adjacent to α 4- α 6 of the WAVE1 meander region (Fig. 3c and supplementary Fig. 14). Furthermore, truncation of α 6 (154_{WAVE1}-WRC) also decreases Rac1 binding (Fig. 3c and supplementary Fig. 13), suggesting that the helix or adjacent parts of the meander may contact the bound GTPase directly or stabilize its interaction sites on Sra1. These data implicate a Rac1 binding site on the WRC involving an Sra1 surface and perhaps part of the meander region of WAVE1. Interactions of Rac1 could then trigger conformational changes in the meander region and/or its contact site on Sra1. Since the meander appears to cooperatively stabilize the V- and C-regions of WAVE1 (see above), these perturbations could drive WRC activation by causing release of the VCA.

Activation by phosphorylation

In cells, phosphorylation of the meander region modulates WRC activity. Several groups report that phosphorylation of the strictly conserved Tyr 150 of WAVE2 (Tyr 151 in WAVE1 and WAVE3) by the Abl kinase is important for WRC-mediated actin assembly

and lamellipodia formation¹⁵⁻¹⁷. Additionally, phosphorylation of WAVE Tyr 125 by Src or Thr 138 by Cdk5, alters cellular actin dynamics^{18,19}.

Tyr 151 of WAVE1 is located in the $\alpha 5$ - $\alpha 6$ loop of the meander region, and is buried in a hydrophobic pocket formed by Sra1 and WAVE1 (Fig. 3c and Supplementary Fig 9). Phosphorylation of Tyr 151 would thus disrupt the contacts between the meander region and Sra1, leading to destabilization of the C-helix of the VCA motif and WRC activation. To test this idea, we reconstituted a miniWRC containing a phospho-mimicking Y151E mutation *in vitro*, and generated the analogous full-length WRC in HeLa cells using a knock down/reexpression strategy. Consistent with the structural predictions, the mutant complexes displayed high actin assembly activity both *in vivo* and *in vitro* (Figs. 3a and 3d). Mutation of the Y151-binding pocket in Sra1 (F686_{ESra1}-miniWRC) equivalently activates the WRC (Fig. 3d).

Tyr 125 of WAVE1 is also strictly conserved from animals to plants (Supplementary Fig. 8). This residue is located in $\alpha 3$ and its side chain packs against Gln 685 and makes a hydrogen bond to Asp 689 of Sra1 (Fig 3c and Supplementary Fig. 9). Phosphorylation of Tyr 125 should disrupt the contact with Asp 689, and could destabilize the meander region of WAVE1, leading to release of the VCA. Consistent with this, replacement of WAVE2 with a Y124D mutant in cells increased lamellipodia formation (Fig. 3a). Thr 138 of WAVE1 makes intramolecular contacts with $\alpha 4$ and $\alpha 5$; its hydroxyl group is part of a network of hydrogen bonds that span between these secondary elements (Fig. 3c and Supplementary Fig. 9). Phosphorylation of Thr 138 may thus also perturb the structure of the meander region, again contributing to activation of the WRC^{18,19}.

Together, the data suggest that, analogous to Rac1 activation, phosphorylation could destabilize the meander region and/or its interactions with Sra1, leading to release of the VCA and activation of the WRC.

Discussion

The WRC is typically clustered to high density at its sites of action in cells. This is believed to be necessary for spatially restricted actin assembly during, for example, polarized cell movement¹. Clustering is mediated by the combined actions of phosphoinositide lipids and Rac, as well as various SH3 containing proteins^{1,3}. The polybasic region of WAVE2 (equivalent to residues 172-184 of WAVE1) can bind phosphoinositide lipids *in vitro*, and is essential for membrane recruitment of the WRC and formation of lamellipodia in cells¹². Surface electrostatic calculations show that the face containing the WAVE1:Abi2:HSPC300 four-helix bundle is negatively charged (Fig. 4a), while much of the face of the complex adjacent to the polybasic region is positively charged (Fig. 4b). This polar distribution suggests that when the WRC is recruited to the plasma membrane, the side covered by the four-helix bundle is exposed to the cytoplasm, while the opposite side contacts the membrane. In this orientation Rac would bind approximately to the side of the WRC (Fig. 4c), and its C-terminal isoprene group, the polybasic region of WAVE and the basic surface of the Sra1/Nap1 dimer could all be directed toward the plasma membrane. The meander region and the VCA motif of WAVE would face the cytoplasm, making them accessible to

other regulators (e.g. kinases), and to the Arp2/3 complex and actin. This organization would allow simultaneous phosphoinositide and Rac binding, cooperatively recruiting the WRC to membranes and enhancing allosteric activation. Self-association of the WRC at membranes¹⁴, and consequent enhanced activity⁵, could be mediated by inter-complex binding of the N-terminal helix of Sra1 with the WAVE/Abi/HSPC300 trimer, as observed in the crystal lattice (Supplementary Fig. 3).

Sra1 was recently reported to support translation inhibition through simultaneous binding to the translational regulator, FMRP, and the translation initiation factor, eIF4E^{9,10}. However, the putative mode of eIF4e binding is incompatible with the WRC structure (Fig. 1b, Supplementary Fig. 15). Thus, eIF4E may bind to isolated Sra1, but not the WRC, consistent with the finding that eIF4E co-immunoprecipitates with Sra1 but not WAVE⁹. These observations suggest that Sra1 may partition between the WRC, which regulates actin dynamics, and a free (or alternatively complexed) state, which regulates translation. Similar arguments have also been made regarding different pools of Nap1³² and Abi³³. Interestingly, defects in Sra1 or its ligands in both pathways—protocadherin-10 which binds the WRC³⁴, and FMRP—are implicated in autism and other mental disorders^{35,36}, suggesting that an appropriate balance of these pathways or their joint action may be needed for proper neuronal development and function. Future studies of the intact WRC and its separate components will reveal how this system coordinates multiple processes in normal and abnormal cellular function.

Methods summary

Sra1, Nap1, WAVE1, Abi2 and HSPC300 were overexpressed separately, partially purified, assembled into an Sra1:Nap1 dimer and a WAVE1/Abi2/HSPC300 trimer, respectively, and then assembled into the miniWRC pentamer. Further purification produced homogenous samples. Crystals of miniWRC were obtained by hanging-drop vapor-diffusion at 4 °C. All the data sets were collected at the ID-19 beamline (APS, Chicago) and processed with the HKL3000 suite³⁷ and CCP4 suites³⁸. Experimental phases were determined from Se-MIRAS data collected on samples containing either SeMet-Sra1 or SeMet-Nap1, and analyzed using ShelxD. Phases were improved using MLPHARE and Parrot. The atomic model of the complex was built using Buccaneer and Coot, and refined using Refmac 5. Equilibrium dialysis was done at room temperature and protein concentrations were determined using Deep Purple gel staining (GE Healthcare). Actin polymerization and GST-Rac1 pull-down assays were performed as described previously¹³. HeLa cells were grown directly on coverslips, fixed in 4% paraformaldehyde, and prepared for immunofluorescence as described²⁵.

Supplementary Material

Refer to Web version on PubMed Central for supplementary material.

Acknowledgments

We thank Baoyu Chen for providing samples of full-length WRC and VCA polypeptide for EM and some biochemical analyses, Chi Pak for helping with the TIRF experiment, Diana Tomchick and Chad Brautigam for

technical assistance and Nick Grishin for assistance with sequence analysis and discussion. Research was supported by fellowships from the Cancer Research Institute and NIH (1F32-GM06917902) to Z.C. and S.B.P., respectively, an Allergic Diseases Training grant (AI07047) to T.S.G., grants from the NIH to D.D.B. (R01-AI065474), Z.O. (R01-GM053163) and M.K.R. (R01-GM056322), a grant from the Welch Foundation to M.K.R. (I-1544) and the Howard Hughes Medical Institute. D.D.B. is a Leukemia and Lymphoma Society Scholar. Use of Argonne National Laboratory Structural Biology Center beamlines at the Advanced Photon Source was supported by the U.S. D.O.E. under contract DE-AC02-06CH11357.

References

1. Takenawa T, Suetsugu S. The WASP-WAVE protein network: connecting the membrane to the cytoskeleton. *Nat Rev Mol Cell Biol.* 2007; 8:37–48. [PubMed: 17183359]
2. Pollitt AY, Insall RH. WASP and SCAR/WAVE proteins: the drivers of actin assembly. *J Cell Sci.* 2009; 122:2575–2578. [PubMed: 19625501]
3. Padrick SB, Rosen MK. Physical mechanisms of signal integration by WASP family proteins. *Annu Rev Biochem.* 2010; 79:707–735. [PubMed: 20533885]
4. Kim AS, Kakalis LT, Abdul-Manan N, Liu GA, Rosen MK. Autoinhibition and activation mechanisms of the Wiskott-Aldrich syndrome protein. *Nature.* 2000; 404:151–158. [PubMed: 10724160]
5. Padrick SB, et al. Hierarchical regulation of WASP/WAVE proteins. *Mol Cell.* 2008; 32:426–438. [PubMed: 18995840]
6. Eden S, Rohatgi R, Podtelejnikov AV, Mann M, Kirschner MW. Mechanism of regulation of WAVE1-induced actin nucleation by Rac1 and Nck. *Nature.* 2002; 418:790–793. [PubMed: 12181570]
7. Stovold CF, Millard TH, Machesky LM. Inclusion of Scar/WAVE3 in a similar complex to Scar/WAVE1 and 2. *BMC Cell Biol.* 2005; 6:11. [PubMed: 15752430]
8. Vartiainen MK, Machesky LM. The WASP-Arp2/3 pathway: genetic insights. *Curr Opin Cell Biol.* 2004; 16:174–181. [PubMed: 15196561]
9. Napoli I, et al. The fragile X syndrome protein represses activity-dependent translation through CYFIP1, a new 4E-BP. *Cell.* 2008; 134:1042–1054. [PubMed: 18805096]
10. Schenck A, et al. CYFIP/Sra-1 controls neuronal connectivity in *Drosophila* and links the Rac1 GTPase pathway to the fragile X protein. *Neuron.* 2003; 38:887–898. [PubMed: 12818175]
11. Kobayashi K, et al. p140Sra-1 (specifically Rac1-associated protein) is a novel specific target for Rac1 small GTPase. *J Biol Chem.* 1998; 273:291–295. [PubMed: 9417078]
12. Oikawa T, et al. PtdIns(3,4,5)P3 binding is necessary for WAVE2-induced formation of lamellipodia. *Nat Cell Biol.* 2004; 6:420–426. [PubMed: 15107862]
13. Ismail AM, Padrick SB, Chen B, Umetani J, Rosen MK. The WAVE regulatory complex is inhibited. *Nat Struct Mol Biol.* 2009; 16:561–563. [PubMed: 19363480]
14. Lebensohn AM, Kirschner MW. Activation of the WAVE complex by coincident signals controls actin assembly. *Mol Cell.* 2009; 36:512–524. [PubMed: 19917258]
15. Sossey-Alaoui K, Li X, Cowell JK. c-Abl-mediated phosphorylation of WAVE3 is required for lamellipodia formation and cell migration. *J Biol Chem.* 2007; 282:26257–26265. [PubMed: 17623672]
16. Stuart JR, Gonzalez FH, Kawai H, Yuan ZM. c-Abl interacts with the WAVE2 signaling complex to induce membrane ruffling and cell spreading. *J Biol Chem.* 2006; 281:31290–31297. [PubMed: 16899465]
17. Leng Y, et al. Abelson-interactor-1 promotes WAVE2 membrane translocation and Abelson-mediated tyrosine phosphorylation required for WAVE2 activation. *Proc Natl Acad Sci U S A.* 2005; 102:1098–1103. [PubMed: 15657136]
18. Miyamoto Y, Yamauchi J, Tanoue A. Cdk5 phosphorylation of WAVE2 regulates oligodendrocyte precursor cell migration through nonreceptor tyrosine kinase Fyn. *J Neurosci.* 2008; 28:8326–8337. [PubMed: 18701695]
19. Ardern H, et al. Src-dependent phosphorylation of Scar1 promotes its association with the Arp2/3 complex. *Cell Motil Cytoskeleton.* 2006; 63:6–13. [PubMed: 16317717]

20. Dai Z, Pendergast AM. Abi-2, a novel SH3-containing protein interacts with the c-Abl tyrosine kinase and modulates c-Abl transforming activity. *Genes Dev.* 1995; 9:2569–2582. [PubMed: 7590236]
21. Holm L, Kaariainen S, Rosenstrom P, Schenkel A. Searching protein structure databases with DaliLite v.3. *Bioinformatics.* 2008; 24:2780–2781. [PubMed: 18818215]
22. Soding J, Biegert A, Lupas AN. The HHpred interactive server for protein homology detection and structure prediction. *Nucleic Acids Res.* 2005; 33:W244–248. [PubMed: 15980461]
23. Jia D, et al. WASH and WAVE actin regulators of the Wiskott-Aldrich syndrome protein (WASP) family are controlled by analogous structurally related complexes. *Proc Natl Acad Sci U S A.* 2010; 107:10442–10447. [PubMed: 20498093]
24. Derivery E, et al. The Arp2/3 activator WASH controls the fission of endosomes through a large multiprotein complex. *Dev Cell.* 2009; 17:712–723. [PubMed: 19922875]
25. Gomez TS, Billadeau DD. A FAM21-containing WASH complex regulates retromer-dependent sorting. *Dev Cell.* 2009; 17:699–711. [PubMed: 19922874]
26. Goley ED, Rodenbusch SE, Martin AC, Welch MD. Critical conformational changes in the Arp2/3 complex are induced by nucleotide and nucleation promoting factor. *Mol Cell.* 2004; 16:269–279. [PubMed: 15494313]
27. Marchand JB, Kaiser DA, Pollard TD, Higgs HN. Interaction of WASP/Scar proteins with actin and vertebrate Arp2/3 complex. *Nat Cell Biol.* 2001; 3:76–82. [PubMed: 11146629]
28. Chereau D, et al. Actin-bound structures of Wiskott-Aldrich syndrome protein (WASP)-homology domain 2 and the implications for filament assembly. *Proc Natl Acad Sci U S A.* 2005; 102:16644–16649. [PubMed: 16275905]
29. Panchal SC, Kaiser DA, Torres E, Pollard TD, Rosen MK. A conserved amphipathic helix in WASP/Scar proteins is essential for activation of Arp2/3 complex. *Nat Struct Biol.* 2003; 10:591–598. [PubMed: 12872157]
30. Stradal TE, et al. Regulation of actin dynamics by WASP and WAVE family proteins. *Trends Cell Biol.* 2004; 14:303–311. [PubMed: 15183187]
31. Steffen A, et al. Sra-1 and Nap1 link Rac to actin assembly driving lamellipodia formation. *EMBO J.* 2004; 23:749–759. [PubMed: 14765121]
32. Weiner OD, et al. Hem-1 complexes are essential for Rac activation, actin polymerization, and myosin regulation during neutrophil chemotaxis. *PLoS Biol.* 2006; 4:e38. [PubMed: 16417406]
33. Ryu JR, Echarri A, Li R, Pendergast AM. Regulation of cell-cell adhesion by Abi/Diaphanous complexes. *Mol Cell Biol.* 2009; 29:1735–1748. [PubMed: 19158278]
34. Nakao S, Platek A, Hirano S, Takeichi M. Contact-dependent promotion of cell migration by the OL-protocadherin-Nap1 interaction. *J Cell Biol.* 2008; 182:395–410. [PubMed: 18644894]
35. Nowicki ST, et al. The Prader-Willi phenotype of fragile X syndrome. *J Dev Behav Pediatr.* 2007; 28:133–138. [PubMed: 17435464]
36. Stefansson H, et al. Large recurrent microdeletions associated with schizophrenia. *Nature.* 2008; 455:232–236. [PubMed: 18668039]
37. Minor W, Cymborowski M, Otwinowski Z, Chruszcz M. HKL-3000: the integration of data reduction and structure solution—from diffraction images to an initial model in minutes. *Acta Crystallogr D Biol Crystallogr.* 2006; 62:859–866. [PubMed: 16855301]
38. Dodson EJ, Winn M, Ralph A. Collaborative Computational Project, number 4: providing programs for protein crystallography. *Methods Enzymol.* 1997; 277:620–633. [PubMed: 18488327]

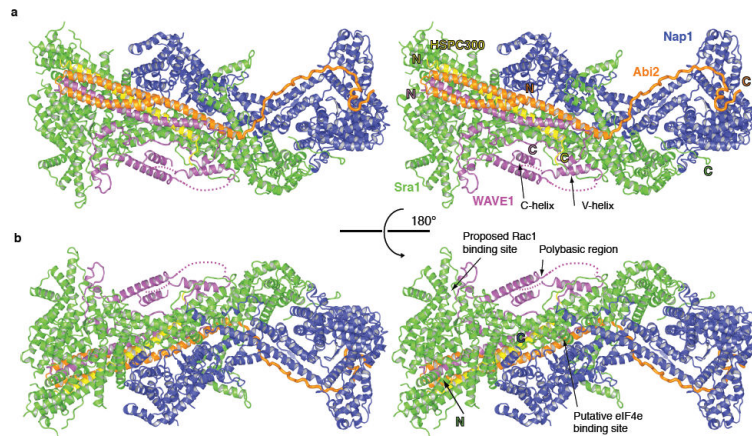


Figure 1. MiniWRC structure

a, Stereo view of miniWRC. Sra1, Nap1, WAVE1, Abi2 and HSPC300 are green, blue, magenta, orange and yellow, respectively. The A-region (residues 545-559), α 6-V region linker (residues 185-485) and sequence connecting V- and C-helices (residues 519-528) are not observed in the electron density. Latter two shown as dashed lines. **b**. 180° rotation about a horizontal axis from **a**. Polybasic region and proposed Rac1 and eIF4E binding sites indicated.

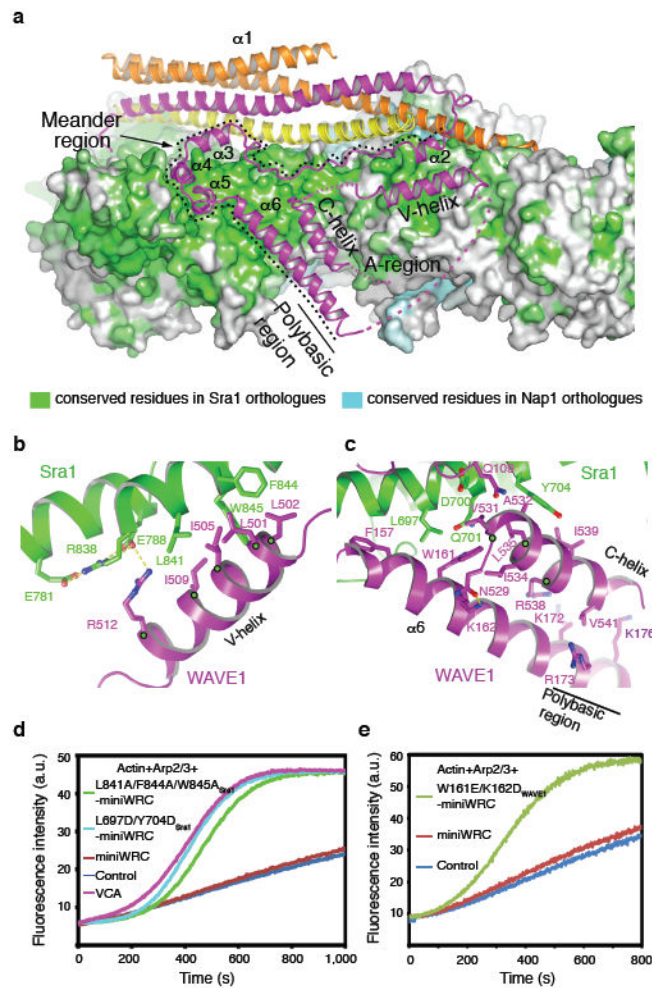


Figure 2. Mechanism of WRC inhibition

a, MiniWRC (rotated 90° about a horizontal axis from Fig. 1a). Sra1 and Nap1 are grey surfaces with conserved residues green and cyan, respectively. Ribbons colored as in Fig. 1. Meander region indicated with dashed line. **b**, V-helix-Sra1 interactions. Hydrogen bonds are dashed. Green dots indicate actin binding residues. **c**, C-helix binding interface. Green dots indicate residues important for Arp2/3 activation. **d**, **e**, Arp2/3-mediated pyrene-actin assembly assays of miniWRC mutants. A.U., arbitrary units. **d**, L697D/Y704D_{Sra1}-miniWRC, L841A/F844A/W845A_{Sra1}-miniWRC, with Sra1 mutated at C- and V-helix binding site, respectively. **e**, W161E/K162D_{WAVE1}-miniWRC, with WAVE1 mutated at C-helix contact site.

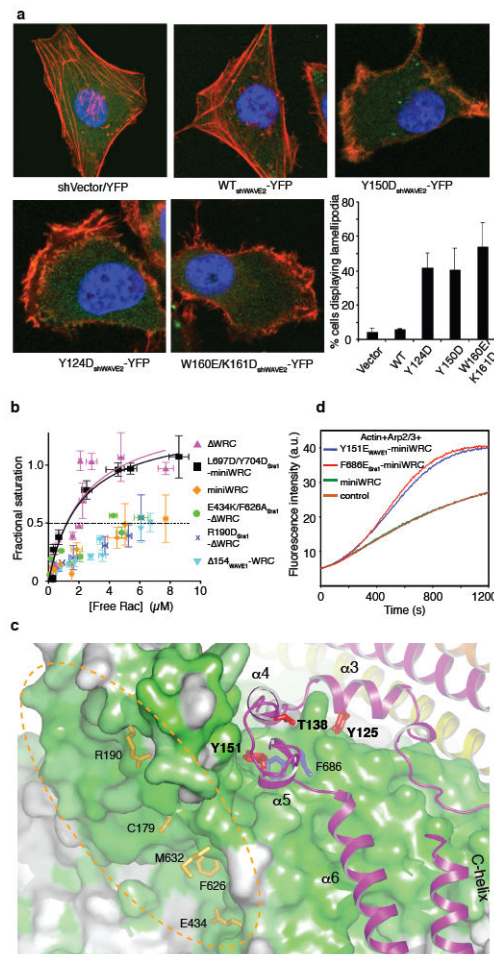


Figure 3. Mechanisms of WRC activation by Rac1 and phosphorylation

a. HeLa cells were transfected with shVector-YFP control, or vectors simultaneously suppressing WAVE2 and expressing shRNA-resistant YFP-tagged WAVE2s (green) and scored blindly for lamellipodial phenotype. F-actin visualized with phalloidin (red). Error bars in lower right panel show standard deviation for at least three independent measurements. **b.** Fractional saturation of WRC versus free Rac1-GMPPNP measured by equilibrium dialysis. Error bars indicate standard deviation in at least two independent measurements. K_D estimated from Rac concentration at 50% saturation; curves are binding isotherms to guide the eye. WRC (containing WAVE1(1-186)) pink triangle, L697D/Y704D_{Sra1}-miniWRC black square, miniWRC gold diamond, E434K/F626A_{Sra1}-WRC green circle, R190D_{Sra1}-WRC blue cross, 154_{WAVE1}-WRC (containing WAVE1(1-154)) cyan inverted triangle. **c.** WAVE1 meander region. Sra1 residues involved in binding Rac1 and WAVE1 Y151 are gold and blue sticks, respectively. Dashed oval indicates proposed Rac1-binding surface. Phosphorylated WAVE1 residues Tyr 125, Thr 138 and Tyr 151 are red sticks. **d.** Arp2/3 mediated pyrene-actin assembly assays with miniWRC (green) or miniWRC containing Y151E_{WAVE1} (blue) or F686E_{Sra1} (red). Control assay (orange) lacked WRC.

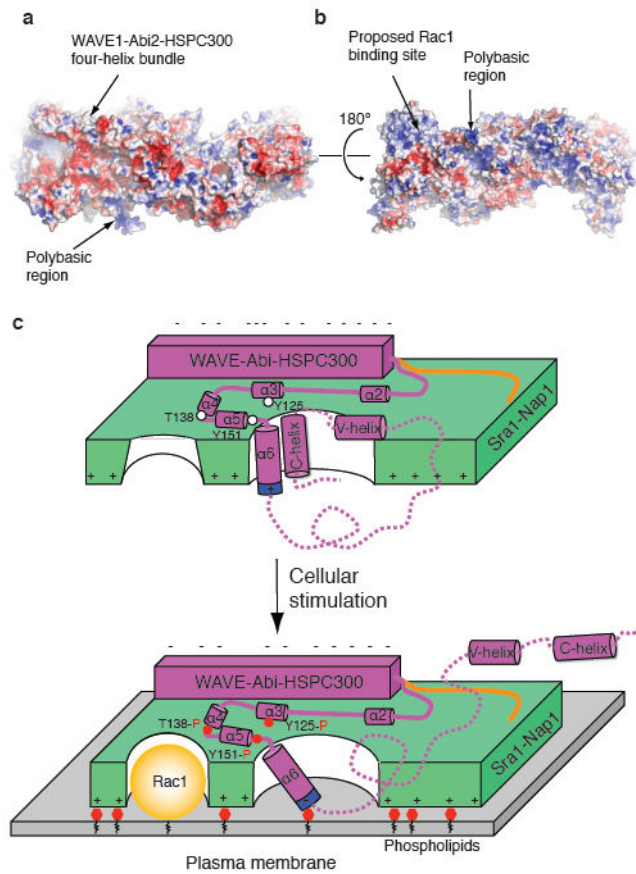


Figure 4. Model for cooperative membrane recruitment and activation of the WRC
a, b Electrostatic surface of miniWRC (red to blue = -5 kT e^{-1} to $+5 \text{ kT e}^{-1}$), oriented as in Figs. 1a and b, respectively. **c**, Schematic illustrating proposed WRC orientation at the plasma membrane and cooperative recruitment and activation by Rac and phospholipids. Phosphorylation sites in WAVE1 meander are indicated. It remains unclear what portions of the meander are disrupted by different stimuli.